Supporting Information

Water-dispersible MnO_2 nanosheets complexed with alginate

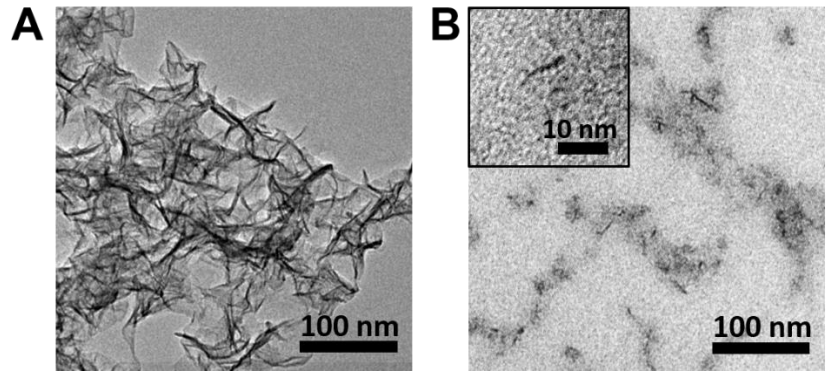

Figure S1. TEM images of (A) alginate-free MnO_2 nanosheets and (B) MnO_2 nanosheets complexed with alginate, denoted as MnO_2 nanosheets.

SEM image of PLGA particles

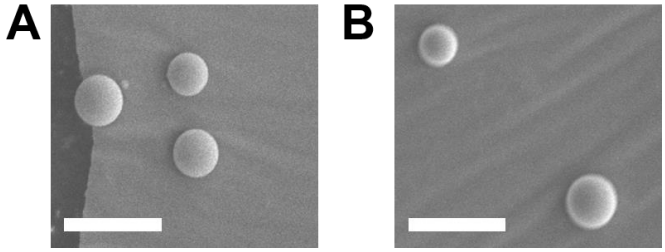

Figure S2. SEM images of (A) PLGA particles and (B) PLGA /MnO_2 particles. Scale bar represents 5 μm.

FTIR spectra of PLGA particle

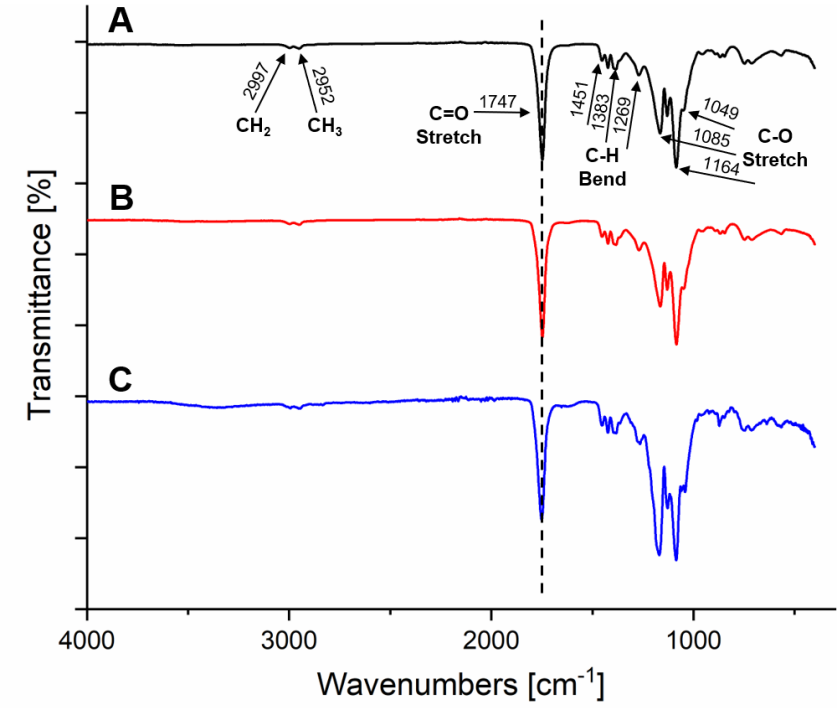

Figure S3. FTIR spectra of (A) Blank PLGA (B) PLGA/MnO_2 (C) PLGA/MnO_2/thrombin particles.

Cumulative O_2 generated through the H_2O_2 decomposition

$$n_{o_2} = \frac{1}{2} \times (initial\ H_2O_2\ concentration\ - final\ H_2O_2\ concentration\ ) \times H_2O_2 volume$$

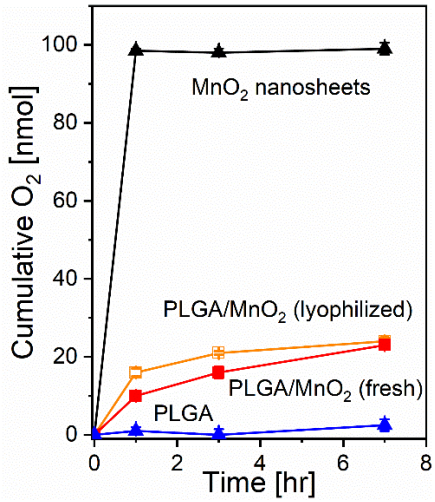

Figure S4. Cumulative O_2 generated through the H_2O_2 decomposition. The cumulative O_2 was quantified by calculating the amount of H_2O_2 that was decomposed. Data points and error bars represent the average and standard deviation of three different samples per condition, respectively.

H_2O_2 decomposition curve under different conditions

(a) Varying initial H_2O_2 concentration

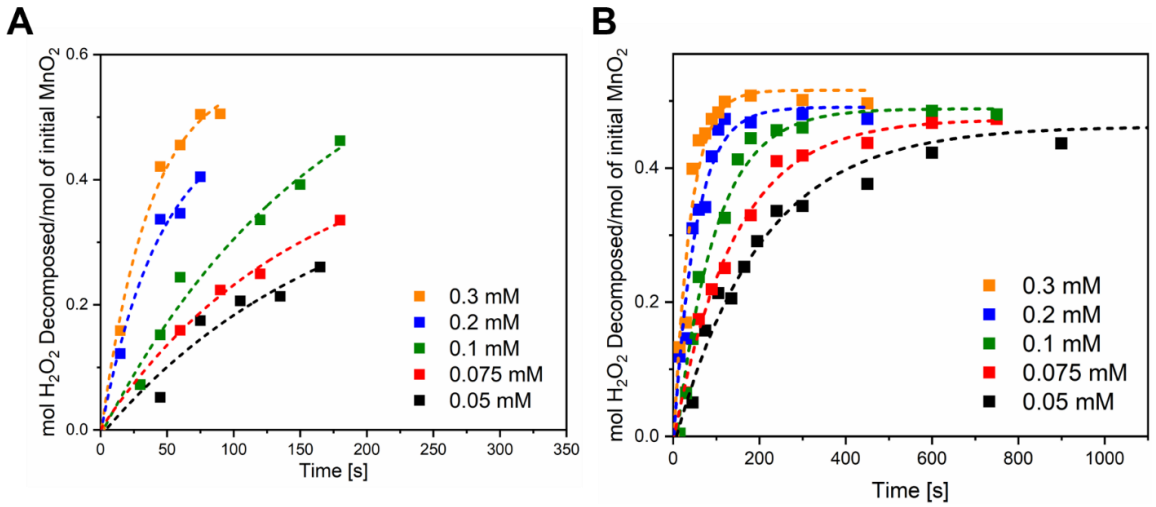

Figure S5. H_2O_2 decomposition curves attained by adding (A) MnO_2 nanosheets and (B) lyophilized PLGA/MnO_2 particles into media with varied H_2O_2 concentrations noted in each figure. Dash lines are for visual guide.

(b) Varying reaction temperature

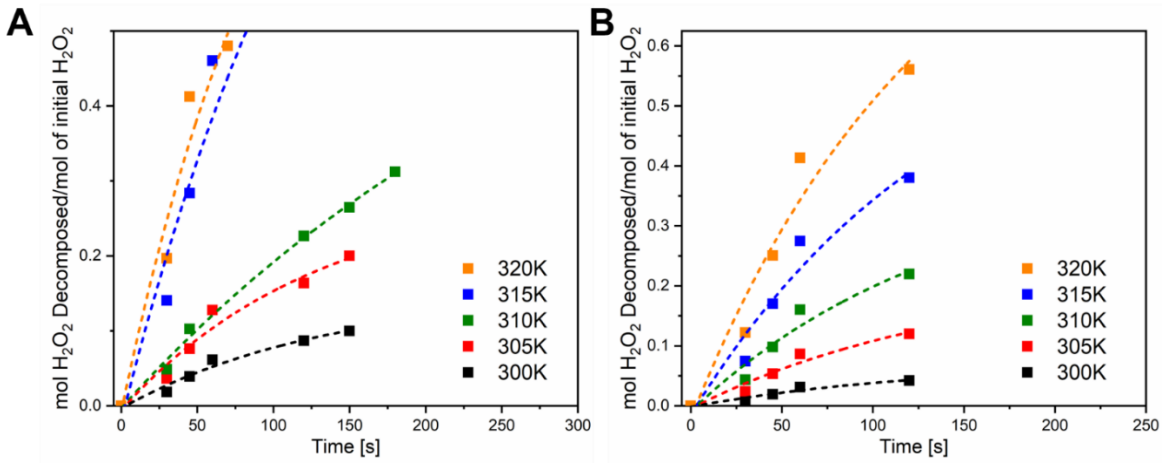

Figure S6. H_2O_2 decomposition curves attained by adding (A) MnO_2 nanosheets and (B) lyophilized PLGA/MnO_2 particles into H_2O_2-containing media under different incubation temperatures noted in each figure. The initial H_2O_2 concentration was kept constant at 0.2 mM. Dash lines are for visual guide.

Theoretical calculation of the difference between internal pressure and external pressure of PLGA/MnO_2 particles

Radius of the PLGA shell: r = 1.6 μm

Radius of the PLGA core: r = 1.5 μm

Density of PLGA polymer: ρ = 1.25 g/ml

Mass per PLGA shell: $M_{PLGA} = \rho \times \frac{4}{3}\pi[(1.6\,\mu m)^3 - (1.5\,\mu m)^3] = 3.77 \times 10^{-12}$ g per particle

Number (*N*) of particles per 10 mg of PLGA polymer: $N_{\text{particle}} = 10\ mg/M_{PLGA} = 2.65 \times 10^9$

Total volume of 10 mg PLGA particle: $V = N_{\text{particle}} \times \frac{4}{3}\pi(1.6\,\mu m)^3 = 45.44\,\mu L$

Mole of O_2 gas generated inside the PLGA particle immersed in 100μM H_2O_2 solution:

$$n_{O_2} = \frac{1}{2} \times (initial\ H_2O_2\ concentration\ - final\ H_2O_2\ concentration\ ) \times H_2O_2 volume$$

Pressure change due to O_2 generation:

$$P_{O_2}V = n_{O_2}RT = P_{O_2} \times 45.44\,\mu L = n_{O_2} \times 0.08206\ atm \cdot Lmol^{-1}K^{-1} \times 310\ K$$

$$\Delta P = \Delta P_{O_2} + \Delta P_{H_2O} \approx \Delta P_{O_2} = P_{O_2} - 0 = P_{O_2}$$

Group	Initial H_2O_2 concentration (μM)	Final H_2O_2 concentration (μM)	Generated O_2 (nmol)	ΔP (mmHg)
Lyophilized PLGA/MnO_2	200	152	24	10.3
Fresh PLGA/MnO_2	200	154	23	9.8
PLGA w/o MnO_2	200	195	2.5	2.1

Table S1. O_2 generation and the pressure change during H_2O_2 decomposition.

Quantitative analysis of fluorescent-labeled MnO_2 intensity change over time

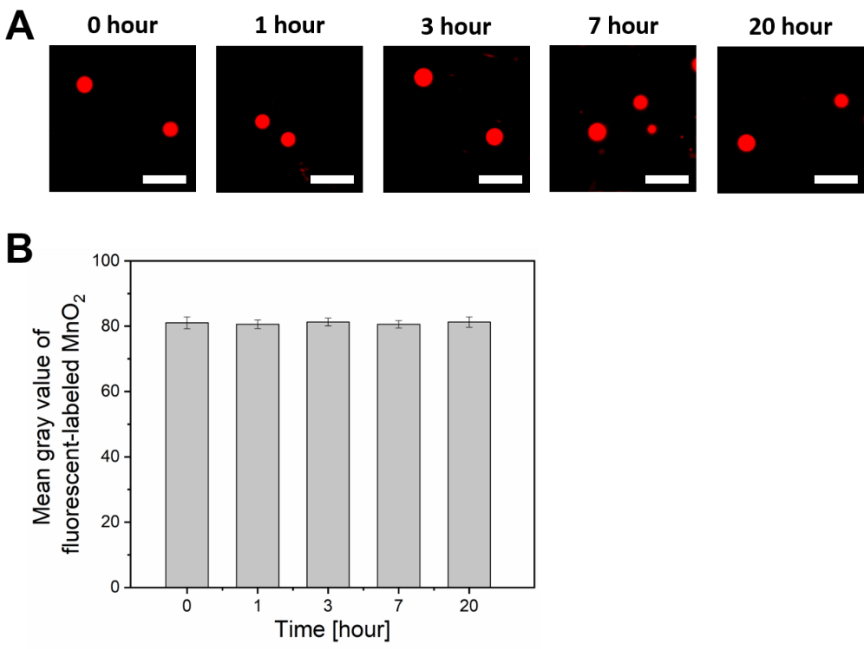

Figure S7. (A) Confocal images of PLGA/MnO_2 microparticles incubated with H_2O_2 at different time points. Alginate associating with MnO_2 nanosheets were labeled with red-colored rhodamine. Scale bar represents 5 μm. (B) Mean gray value of fluorescence from the PLGA/MnO_2 microparticles with H_2O_2 at different time points. Data points and error bars represent the average and standard deviation of three different samples per condition, respectively.

Evaluation of the bio-adhesion of fibrin gel

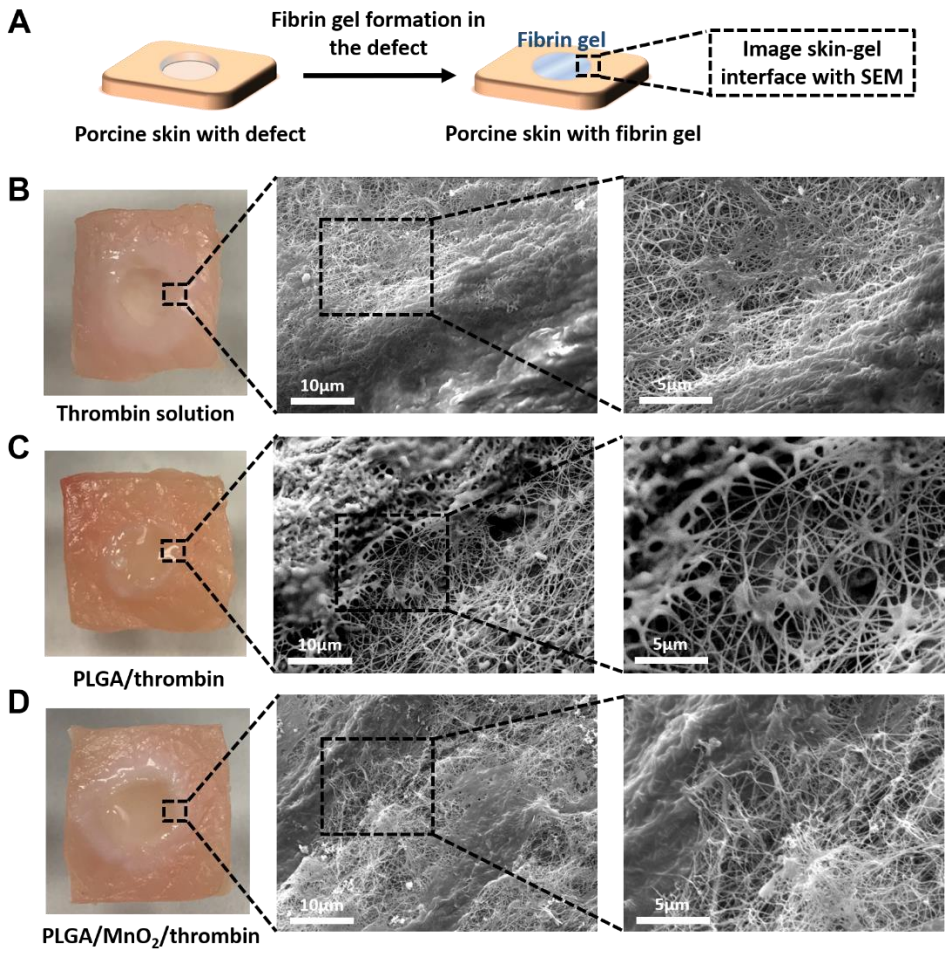

Figure S8. (A) Schematic illustration of the experimental set-up used to evaluate the bio-adhesion of the fibrin gel to a porcine skin explant. The porcine skin explant was punched to simulate wounds where fibrine gels are implanted. The punched wounds were filled with fibrin gels (B-D) SEM images of the interface between skin and fibrin gel. The gel filled a hole created by punching out a center part of the square-shaped porcine skin. (B) Fibrin gel formed by mixing fibrinogen and thrombin solution. (C) Fibrin gel formed by mixing fibrinogen and PLGA/thrombin particles. (D) Fibrin gel formed by mixing fibrinogen and PLGA/MnO_2/thrombin particles.

Evaluation of surface water contact angle of fibrin gel

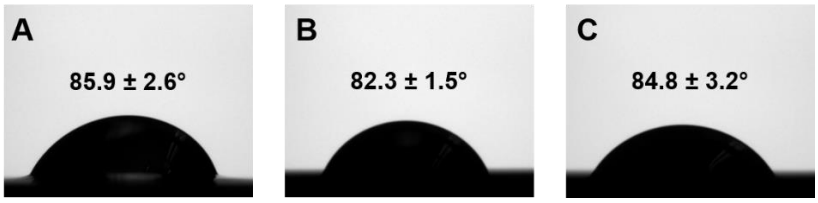

Figure S9. Contact angle measurements were taken with a goniometer using water as the test liquid for gel formed by mixing fibrinogen with (A) thrombin, (B) PLGA/thrombin particles, and (C) PLGA/MnO_2/thrombin particles.

Gelation curve fitting

(1) Single exponential fitting

$G'(t) = G'_{eq} \exp(-\beta/t)$ where $G'(t)$ is the storage modulus, G'_{eq} is the equilibrium storage modulus, β is the characteristic time, and t is time.

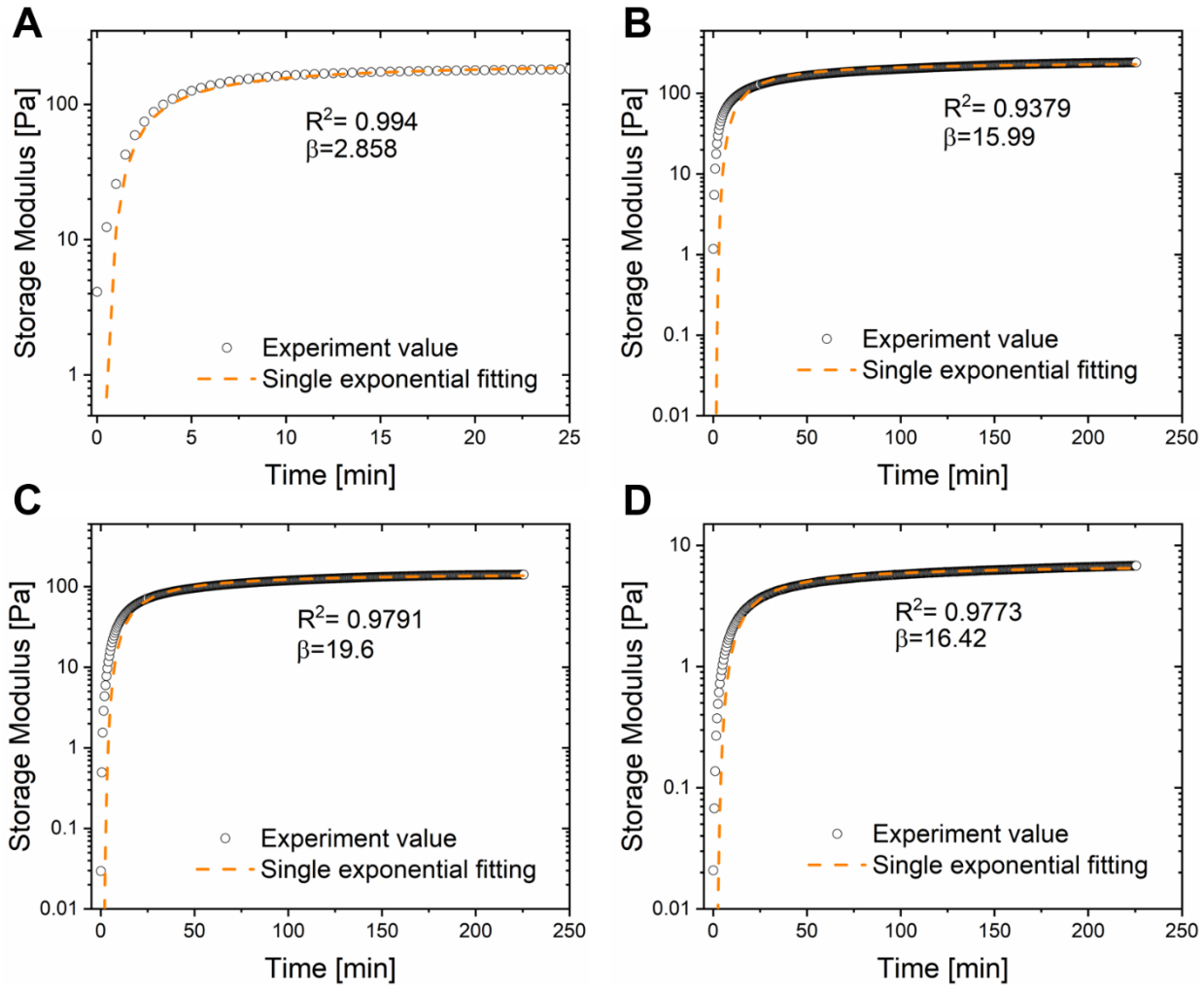

Figure S10. Single exponential fitting of the gelation curve. (A) Gelation curve attained by mixing thrombin solution with fibrinogen solution. (B) Gelation curve attained by mixing PLGA/MnO_2/thrombin particles with a fibrinogen solution. (C) Gelation curve attained by mixing PLGA/thrombin particles with a fibrinogen solution. (D) Gelation curve of the mixture of blank PLGA particles, thrombin solution, and fibrinogen solution.

(2) Double exponential fitting

$G'(t) = G'_0 + G'_1(1 - \exp\left(-\frac{t}{\tau_1}\right)) + G'_2\left(1 - \exp\left(-\frac{t}{\tau_2}\right)\right)$ where $G'(t)$ is the storage modulus; G'_0 is the storage modulus of the pre-gelled solutions; G'_1 is the storage modulus contributed by the first branching and crosslinking reaction phase; G'_2 is the storage modulus caused by the second lateral growth of fibrin polymers; t is the time; and $1/\tau_1$ and $1/\tau_2$ are the characteristic rates for branching and lateral growth, respectively.

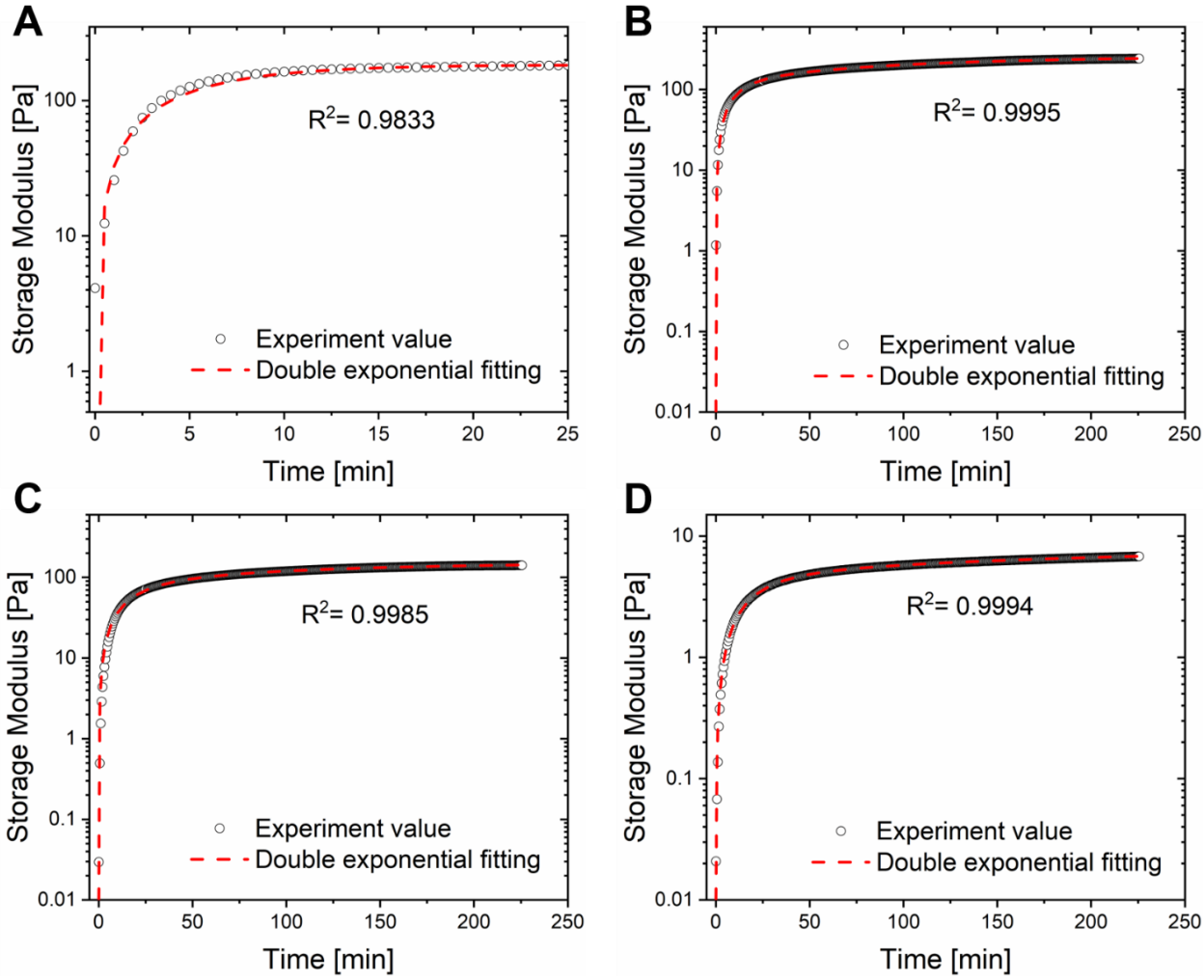

Figure S11. Double exponential fitting of the gelation curve. (A) Gelation curve attained by mixing thrombin solution with fibrinogen solution. (B) Gelation curve attained by mixing

PLGA/MnO_2/thrombin particles with a fibrinogen solution. (C) Gelation curve attained by mixing PLGA/thrombin particles with a fibrinogen solution. (D) Gelation curve of the mixture of blank PLGA particles, thrombin solution, and fibrinogen solution.

In vitro angiogenesis assay

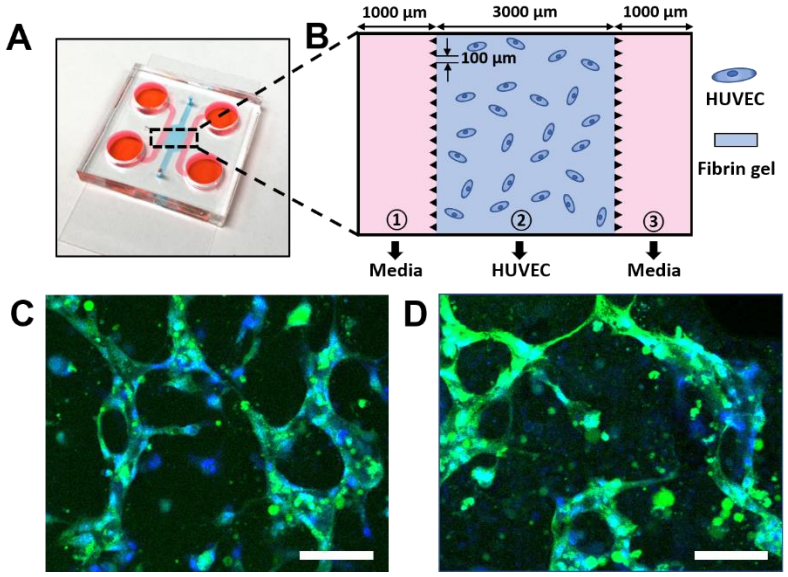

Figure S12. In vitro angiogenesis assay. (A) Schematic illustration of a microfluidic chip device used for the angiogenesis study in vitro. (B) The central portion features three channels. The fibrin gel encapsulating HUVECs filled the center channel ②; cell culture medium filled channels ① and ③. Confocal laser scanning microscopic images of tube formation by human umbilical vein endothelial cells seeded in fibrin gel formed by mixing fibrinogen with (C) thrombin solution and (D) PLGA/MnO_2/thrombin particles. Cells were immunostained with CD31 (in green). Cell nuclei were stained with DAPI (in blue). Scale bar represents 100 μm.

Blood clot formation triggered by thrombin

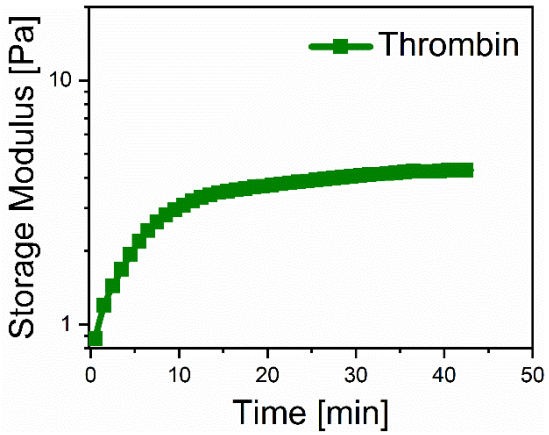

Figure S13. Change in the storage modulus of the blood mixed with a thrombin solution.